

Synthesis of calcium doped strontium barium niobate ceramic samples

G. STANCIU^{a,b,*}, A. ACHIM^a, N. D. SCARISOREANU^a, V. ION^{a,c}, R. BIRJEGA^a, E. ANDRONESCU^b, M. DINESCU^a

^aNational Institute for Lasers, Plasma and Radiation Physics, Magurele, Romania 077125

^bUniversity Politehnica of Bucharest, Faculty of Applied Chemistry and Material Science, Bucharest, Romania, 011061

^cFaculty of Physics, University of Bucharest, 077125 Magurele, Romania

High density polycrystalline $\text{Sr}_x\text{Ba}_{1-x}\text{Nb}_2\text{O}_6$ (SBN) ceramics (with $x = 0.50 \div 0.60$) undoped and Ca doped SBN were obtained by conventional solid-state reaction method. The Ca was used as dopant for increasing the ferroelectric-paraelectric transition temperature, as well as for improving the dielectric leaky behavior of pure SBN. The XRD analysis showed that pure SBN phase is crystallized into a tetragonal tungsten bronze (TTB) structure without secondary phase. Ca doped composition shows a small amount of secondary phase of CaNb_2O_6 . SEM micrographs indicate formation of crystallites with sharp boundaries with an average grain size of about $2 \div 6 \mu\text{m}$ for pure SBN ceramics, while for Ca doped SBN the grains size increases up to $10 \mu\text{m}$. The dielectric characterization shows high dielectric constant values for SBN:50 and SBN:60. Instead, the Ca doping has the effect on the reduction of dielectric constant value, but the dielectric losses are found to be smaller for this composition.

(Received April 22, 2015; accepted May 7, 2015)

Keywords: SBN, CBN, SCBN, TTB structure, Ceramic target, Dielectric properties

1. Introduction

The TB compositions are characterized by the chemical formula $[(A1)_2(A2)_4C_4][(B1)_2(B2)_8]_{30}$, where A1, A2, B and C sites are 15-, 12-, 6- and 9- fold coordinated oxygen octahedral sites in the crystal lattice structure.

The A1 and A2 sites can be occupied by Sr^{2+} , Ba^{2+} , Ca^{2+} , Mg^{2+} , Pb^{2+} , K^+ , Na^+ and some rare earth cations, the B sites by either Nb^{5+} or Ta^{5+} and the C sites are usually empty [1, 2].

Lead-free $\text{Sr}_x\text{Ba}_{1-x}\text{Nb}_2\text{O}_6$ consists of a solid solution between SrNb_2O_6 and BaNb_2O_6 over a wide composition range ($0.25 \leq x \leq 0.75$). The interest in this material is coming from its excellent ferroelectric, pyroelectric, piezoelectric and electro-optic properties [3-5].

For pure SBN the maximum of the phase-transition temperature is in the range $353 \div 358 \text{ K}$ [6]. Such a low Curie temperature implies that SBN is easily depolarized near room temperature, and any potential devices using SBN material will not work properly beyond these temperature values.

Another compound with TTB structure is $\text{Ca}_x\text{Ba}_{1-x}\text{Nb}_2\text{O}_6$ (CBN), which was first mentioned as a ceramic material by Ismailzade in 1959 [7]. CBN offers similar physical properties like SBN, being also well suited for a wide range of applications. The main advantage of CBN compound is the high Curie temperature in the range $523 \div 553 \text{ K}$, higher than that of SBN [5, 8]. Currently, there is a great interest for the processing of oxide materials as thin films with large electro-optic coefficients. These films are promising materials for use in electro-optic (EO) devices like electro-optic waveguide modulators and photorefractive optics.

In this work, the SBN ceramics with different Sr/Ba ratios and calcium-doped SBN, namely $\text{Sr}_xCa_y\text{Ba}_{1-x-y}\text{Nb}_2\text{O}_6$ (SCBN) were obtained and systematically investigated.

2. Experimental

A conventional solid-state method was used to prepare the bulk ceramics with compositions of $\text{Sr}_{0.5}\text{Ba}_{0.5}\text{Nb}_2\text{O}_6$ (SBN:50); $\text{Sr}_{0.6}\text{Ba}_{0.4}\text{Nb}_2\text{O}_6$ (SBN:60) and $\text{Sr}_{0.6}\text{Ca}_{0.28}\text{Ba}_{0.12}\text{Nb}_2\text{O}_6$ (SCBN:60/28). A flow diagram of the experimental procedure is given in Fig. 1. The starting powders were reagent grade SrCO_3 , BaCO_3 , CaCO_3 and Nb_2O_5 as received.

The raw materials were mixed in stoichiometric proportions and homogenized in ethanol medium for 12 h. The slurry was dried at $80 \text{ }^\circ\text{C}$, uniaxially pressed (at 20 MPa) into pellets and calcinated at $1100 \text{ }^\circ\text{C}$ for 6 h in air. Then, the pre-sintered samples were grinded in the agate mortar, the powders were compacted uniaxially (at 20 MPa) into discs with 10 mm diameters and cold isostatically pressed (CIP) at a pressure of 235 MPa for 5 min. All samples were then sintered in air at $1350 \text{ }^\circ\text{C}$ for 10 h to produce dense ceramic pellets.

Differential thermal analysis (DTA) and thermogravimetry (TG) were used to analyze the thermal reaction behavior of the powdered precursors with a heating rate of $10 \text{ }^\circ\text{C} / \text{min}$ in air up to $1400 \text{ }^\circ\text{C}$. Densities of the sintered samples were measured based on the Archimedes principle using xylene as the displacement fluid.

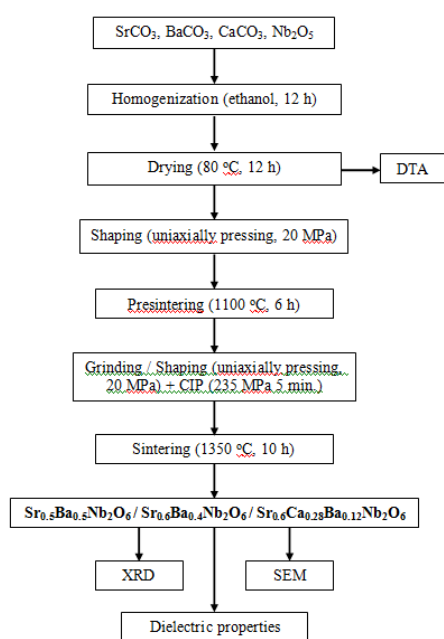


Fig. 1. Flowchart of SBN preparation.

The structure of the ceramic samples was analyzed by x-ray diffraction XRD (PANalytical X'Pert PRO MRD, Netherlands).

Microstructure evolution was observed using a scanning electron microscopy SEM (Quanta Inspect F, Netherlands) with EDAX option. Dielectric properties were analyzed by an impedance gain phase analyzer (HP 4194 A) with a frequency swept in steps from 1 kHz to 1 MHz.

3. Results and discussion

Thermal analysis (DTA and TG curves) of SCBN:60/28 mixture are shown in Fig. 2. It is seen that DTA curve involves two important peaks. The first endothermic one between 700 °C and 830 °C is attributed to the decomposition of the carbonates with a weight loss around 10 %. The second exothermic one between 1000 °C and 1200 °C indicates the formation of SCBN 60/28 compound. The melting point for this composition is about 1400 °C (the last endothermic peak).

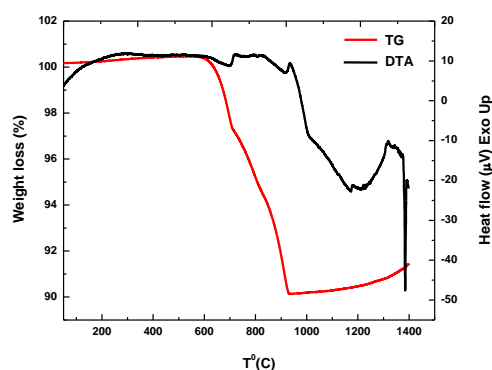


Fig. 2. DTA and TG curves of $\text{Sr}_{0.6}\text{Ca}_{0.28}\text{Ba}_{0.12}\text{Nb}_2\text{O}_6$ precursor powders.

In order to obtain high density ceramics the sintering temperature was selected about of 50 °C below the melting point. The relative density for all three samples was around 98.8 % (of theoretical density).

The XRD spectra on SBN undoped and Ca doped ceramics samples are shown in Fig. 3. For SBN:50 and SBN:60 compositions, all the diffraction peaks indicates that the samples are crystallized into a pure TTB structure without secondary phases. The SCBN:60/28 ceramic sample XRD pattern exhibits a mixture of a TTB major phase with an orthorhombic phase of $(\text{Ba,Ca,Sr})\text{Nb}_2\text{O}_6$ (JCPDS 00-052-1419) and CaNb_2O_6 (JCPDS 00-039-1392).

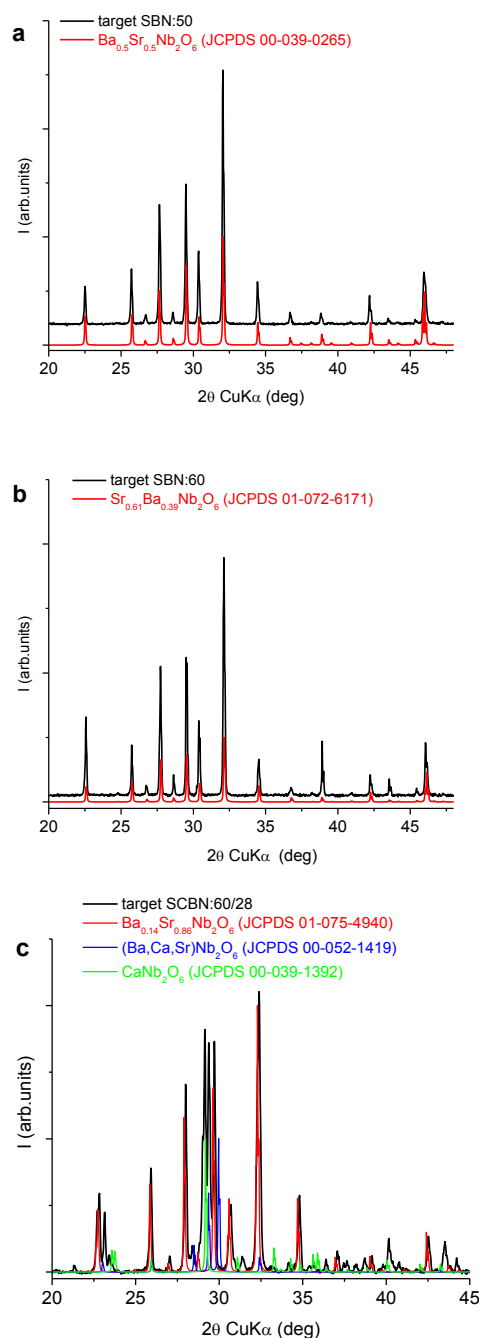


Fig. 3. XRD patterns of SBN ceramics: a) SBN:50; b) SBN:60; c) SCBN:60/28.

The calculated unit cell parameters are presented in Table 1 in comparison with their corresponding JCPDS files. For SBN:50 and SBN:60 ceramics the unit cell parameters values are similar with standard JCPDS values. For SCBN:60/28 sample the unit cell value corresponds to a XRD standard card (JCPDS 01-075-4940) with a significantly low Ba^{2+} content. For this composition in order to obtain a pure TTB structure further refinement of obtaining steps are required.

Table 1. Structural data.

Sample	Cell parameters		
	a (Å)	c (Å)	Vol (Å ³)
target SBN:50	12.485	3.948	615.13
$\text{Sr}_{0.5}\text{Ba}_{0.5}\text{Nb}_2\text{O}_6$ (JCPDS 00-039-0265)	12.465	3.952	614.08
target SBN:60	12.468	3.937	612.02
$\text{Ba}_{0.39}\text{Sr}_{0.61}\text{Nb}_2\text{O}_6$ (JCPDS 01-072-6171)	12.460	3.931	610.40
target SCBN:60/28	12.385	3.914	600.30
$\text{Ba}_{0.14}\text{Sr}_{0.86}\text{Nb}_2\text{O}_6$ (JCPDS 01-075-4940)	12.418	3.907	602.54

Fig. 4 shows the SEM morphology of fractured surfaces of pure SBN and Ca doped SBN. Samples SBN:50 and SBN:60 exhibit well grown grains and clear crystalline boundaries, with an average grain size of about $2 \div 6 \mu\text{m}$, while for SCBN:60/28 compound the grain size increase up to $10 \mu\text{m}$. The abnormal grain growth resulting from locally inhomogeneous compositions is noticed for Ca doped composition.

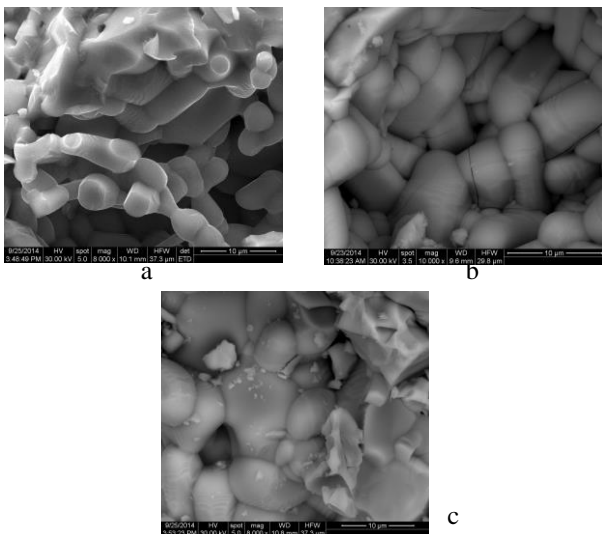


Fig. 4. SEM images of fractured surface of SBN ceramics: a) SBN:50; b) SBN:60; c) SCBN:60/28.

The dielectric constant (ϵ_r) and dielectric loss ($\tan \delta$) values measured at 100 kHz around room temperature are presented in Fig. 5. The dielectric constant value recorded was $\epsilon_r \sim 550$ for SBN:50 and ~ 480 for SBN:60, while the dielectric losses are between $\tan \delta = 0.07 \div 0.08$, in good agreement with the previous reported values [4, 9].

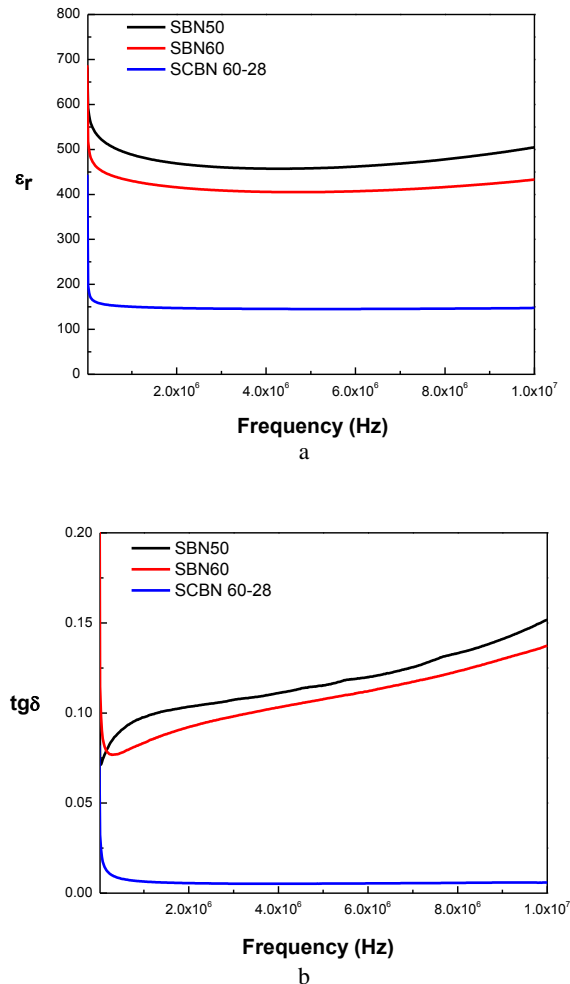


Fig. 5. Dielectric properties ϵ_r (a) and $\tan \delta$ (b) for SBN ceramics.

For SCBN:60/28 composition the dielectric constant values are lower than for undoped SBN $\epsilon_r \sim 170$, but the dielectric losses are smaller ($\tan \delta = 0.01$) for this compound. This value is similar to that reported by X. Han *et. al* for pure CBN [5].

4. Conclusion

High density pellets of $\text{Sr}_x\text{Ba}_{1-x}\text{Nb}_2\text{O}_6$ ceramics ($x = 0.50 \div 0.60$) and Ca doped $\text{Sr}_x\text{Ba}_{1-x}\text{Nb}_2\text{O}_6$ with tungsten-bronze crystalline structure have been obtained. The ceramic samples were prepared by the conventional mixed-oxides method. The phase structure, microstructure and dielectric properties of prepared ceramics as a function

of Sr/Ba ratio and Ca content were investigated. The XRD results showed that pure SBN phase with tungsten bronze structure could be obtained from the solid solutions of SrNb_2O_6 and BaNb_2O_6 . Ca doping leads to the occurrence of secondary phases in $\text{Sr}_{0.6}\text{Ca}_{0.28}\text{Ba}_{0.12}\text{Nb}_2\text{O}_6$ composition. Also, the SEM images show a grain size larger than pure SBN. The dielectric constant value (ϵ_r) is higher for undoped SBN ceramics. However, the dielectric losses ($\tan \delta$) are lower for SCBN composition, an important issue for this type of materials. Finally, these compositions are suitable to be used as ceramic target for obtain thin layers based on pure and Ca doped $\text{Sr}_x\text{Ba}_{1-x}\text{Nb}_2\text{O}_6$.

Acknowledgements

*This work has been funded by the Sectoral Operational Programme Human Resources Development 2007-2013 of the Ministry of European Funds through the Financial Agreement POSDRU/159/1.5/S/132397.

V. Ion was supported by the strategic grant POSDRU/159/1.5/S/137750, "Project Doctoral and Postdoctoral programs support for increased competitiveness in Exact Sciences research" cofinanced by the European Social Fund within the Sectorial Operational Program Human Resources Development 2007–2013.

References

- [1] Marcin Stachowicz, Olga Gawryszewska, Marek A. Swirkowicz, Tadeusz Lukasiewicz, *Acta Cryst.* **E69**, i69–i70, (2013).
- [2] Lingling Wei, Zupei Yang, Xiaolian Chao, Huan Jiao, *Ceramics International* **40**, 5447 (2014).
- [3] Takuma Takahashi, Satoshi Tanaka, Zenji Kato, Keizo Uematsu, *Journal of the Ceramic Society of Japan* **121**(5), 411 (2013).
- [4] Jing Zhang, Genshui Wang, Feng Gao, Chaoliang Mao, Fei Cao, Xianlin Dong, *Ceramics International* **39**, 1971 (2013).
- [5] Xiaokun Han, Lingling Wei, Zupei Yang, Ting Zhang, *Ceramics International* **39**, 4853 (2013).
- [6] Theo Woike, Vaclav Petricek, Michal Dusek, Niels K. Hansen, Pierre Fertey, Claude Lecomte, Alla Arakcheeva, Gervais Chapuis, Mirco Imlau and Rainer Pankrath, *Acta Cryst.* **B59**, 28 (2003).
- [7] I. G. Ismailzade, *Kristallografiya* **5**, 268, (1960).
- [8] Alexander Niemer, Rainer Pankrath, Klaus Betzler, Manfred Burianek, Manfred Muehlberg, *World Journal of Condensed Matter Physics* **2**, 80 (2012).
- [9] P. K. Patro, A. R. Kulkarni, S. M. Gupta, C. S. Harendranath, *Defence Science Journal* **57**(1), 79 (2007).

*Corresponding author: george.stanciu@inflpr.ro